Carbohydrate Polymers 92 (2013) 2314–2320

Contents lists available at SciVerse ScienceDirect

Carbohydrate Polymers

journal homepage: www.elsevier.com/locate/carbpol

Synthesis and swelling properties of β-cyclodextrin-based superabsorbent resin with network structure

Zhanhua Huang*, Shouxin Liu, Guizhen Fang, Bin Zhang

Key laboratory of Bio-based Material Science and Technology of Ministry of Education, Northeast Forestry University, Harbin 150040, China

ARTICLE INFO

Article history:
Received 25 February 2012
Received in revised form
28 September 2012
Accepted 3 December 2012
Available online 12 December 2012

Keywords:
β-cyclodextrin
Superabsorbent
Biodegradable
Salt resistance
Three-dimensional network structure

ABSTRACT

A biodegradable, β-cyclodextrin-based superabsorbent resin was synthesized by the inverse suspension method. The microstructure, chemical structure, and thermal performance of the resin were characterized by scanning electron microscopy, Fourier transform-infrared spectroscopy, and differential scanning calorimetry. The effects of the synthesis conditions (dosage of cross-linking agent, mass ratios of acrylic acid to acrylamide, mass ratios of β-cyclodextrin to total monomer, neutralization degree, initiator dosage, and reaction time) were optimized to achieve a resin with a maximum swelling capacity. The water absorbency of the optimized resin in distilled water was 1544.76 g/g and that in 0.9 wt.% NaCl was 144.52 g/g. The resin, which is thermoplastic as well as pH-sensitive, had good salt resistance and underwent a maximum in swelling with time in $CaCl_2$ and $AlCl_3$ solutions. The fracture surface of the dry resin contained many pores. After swelling, the internal hydrogel showed a typical three-dimensional network structure. The biodegradation of the resin reached 71.2% after 18 days treatment at 30 °C with *Lentinus edodes*.

1. Introduction

Super absorbent polymers (SAP) are a new type of functional polymer that has been developed in recent years. This material can absorb water at hundreds or even thousands of times of its weight. SAP, with its super water absorbency and retention, have wide applications in areas including personal health products, civil construction, industrial and agricultural production, and medical materials (Silberbush, Adar, & De, 1993; Zhang & Li, 2005; Sun et al., 2006; Liu, Zhang, & Zhu, 2008; Wang, Zhang, & Wang, 2008). Furthermore, SAP can be used in industries dealing with food crops, cash crops, flower vegetables, forest, lawn cultivation, and desert improvement because of its super water absorbency and retention. Thus, SAP is gradually becoming an important part of the agricultural technology system with excellent water-saving abilities (Han, Yang, & Luo, 2010; Yao & Zhou, 2003; Abedi-Koupai, Eslamian, & Asadkazami, 2008; Bhardwaj, Shainberg, Goldstein, Warrington, & Levy, 2007). In addition, a number of studies are being conducted on the use of SAP as a waterproofing agent in communication cables, humidity regulator, active enzyme carrier, artificial snow, and so on (Ficarra et al., 2002; Kabiri, Omidian, Hashemi, & Zohuriaan-Mehr, 2003).

SAP, can be classified into two types depending on their raw material source. Polymerized resins that are based on petrochemical products such as acrylic acid, acrylamide, polyvinyl alcohol, and acrylonitrile. This type has better water absorbency, but has poorer penetration performance, is more expensive and is nonbiodegradable. The biodegradable resins that are synthesized from natural polymers such as starch, cellulose, chitosan are the second type of SAP. Although this type is biodegradable, their water absorption and retention performance are poorer. Therefore, the preparation of SAP with super water absorbency, excellent machinery performance, and low cost through the modification of natural polymers by copolymerization is a popular area of research (Chang, Duan, Cai, & Zhang, 2010; Buchholz, 1996).

β-cyclodextrin (β-CD), a cyclic oligosaccharide composed of seven glucose molecules with α-1,4-glucosidase linkages, is produced from amylose by cyclodextrin glucosyltransferase from *Bacillus*, which has a micro-environment of a chiral, hydrophilic outside and a hydrophobic interior cavity (Szejtli, 1998; Dell Valle, 2004). Previous studies have focused on the use of the β-CD structure in forming inclusion compounds that are mainly used for organic compound adsorption and applications in fields dealing with environmental protection, cosmetics, slow-release drugs, and so on (Banerjee & Chen, 2010; Cobos, Martinez Perez, Monreal Romero, & Garcia Casillas, 2007; Guo & Jiang, 2007). β-CD is biodegradable and contains a number of alcoholic hydroxyl groups for chemical reactions such as etherification, esterification, oxidation, cross-linking, and so on (Dell Valle, 2004). β-CD is suitable

* Corresponding author. Tel.: +86 451 82192905.
E-mail address: huangzh1975@163.com (Z. Huang).

0144-8617/$ – see front matter © 2012 Elsevier Ltd. All rights reserved.
http://dx.doi.org/10.1016/j.carbpol.2012.12.002

as starting material for the synthesis of SAP due to the abundant hydrophilic hydroxyl group. However, the molecular weight of β-CD is low. In order to increase molecular weight of the product, hydrophilic monomer could be link with β-CD by chemical cross-linking reactions. Meanwhile, the cyclic oligosaccharide chemical structure of β-CD could increase three-dimensional network structure of product in cross-linking reactions, favoring the swelling capacity of the product.

In the present study, we took advantage of the β-CD chemical structure with many hydroxyl groups, and we synthesized SAP with three-dimensional interpenetrating network structure, which have several advantages such as superior water absorption ability, excellent salt resistance, and biological degradation through self-assembly graft polymerization. We studied the influence of reaction factors, such as initiator dosage, reaction time, temperature, and raw materials ratio on the swelling capacity of the resin. The chemical and surface structures of the products were characterized, and their biodegradability in fungi and thermal performance were determined and discussed.

2. Experimental

2.1. Materials

β-CD, acrylic acid (AA), N,N′-methylenebisacrylamide (NMBA), acrylamide (AM), $K_2S_2O_8$, NaCl, $CaCl_2$, and $AlCl_3$, were purchased from the chemical reagent development center of Kemiou Engineering (Tianjin, China). *Penicillium*, *Aspergillus niger* (*A. niger*), and *Lentinus edodes* (*L. edodes*) were obtained from the Laboratory of Forest Protection of Northeast Forestry University. All agents used were of analytical grade, and all solutions were prepared with distilled water.

2.2. Synthesis of β-CD-based resin

Cyclohexane (50 mL) and arlacel-80 (10 mL) were mixed in a 250 mL four-neck reaction bottle. Nitrogen flowed through for 10 min, and the reaction temperature was raised to 65 °C. Afterwards, β-CD, AA, and AM were added based on their mass ratio. NaOH (1 mol/L) solution was used to adjust the mixture to a specified degree of neutralization. The mixture was uniformly mixed to dissolve the solid samples. $K_2S_2O_8$ (quantitative initiator) and NMBA (cross-linking agent) were then added dropwise using a funnel at a constant rate of 1–2 d/s with stirring. The mixture reacted under nitrogen protection. The temperature was maintained for 0.5 h after the reaction. The mixture passed through a filter, and the filtered cake was dried at 50 °C for 48 h until a constant weight was obtained. The cyclohexane filtrate was recycled to achieve granular resin products. A range of products were obtained by changing the reaction factors such as the mass ratio of β-CD, AA, and AM, the dosages of $K_2S_2O_8$ and NMBA, reaction time, and neutralization degree. The optimum synthesis conditions for the super absorbent resin were explored using water absorbency in distilled water and saline solution as the evaluation indicator.

2.3. Characterization

The Fourier transform-infrared (FTIR) spectrum was obtained from a MAGNA 560 FTIR spectrometer (Thermo Nicolet Corporation, USA) using KBr discs in the range from 4000 cm^{-1} to 400 cm^{-1}. Scanning electron microscopy (SEM) images were obtained using a FEI QUANTA 200 microscope. The swollen resin hydrogel were frozen in liquid nitrogen and immediately snapped and freeze-dried. The fractured surface of the resin hydrogel was observed. Differential scanning calorimetry (DSC) was done using a DSC2004 heat flux differential scanning calorimeter (NETZSCH, Germany) at a temperature range from 293 K to 773 K with a heating rate of 10 K/min and an argon gas flow at 40 mL/min.

2.4. Swelling and absorbency of resins in chloride and pH buffer solutions

NaCl, $CaCl_2$, and $AlCl_3$ solutions were prepared at different concentrations (0.1 mol/L, 0.05 mol/L, and 0.01 mol/L), where 0.1 g of the resin products was mixed with 200 mL of each salt solution. The water absorbency was measured. Buffer solutions with pH values of 2, 4, 6, 8, 10, and 12 were prepared, where 0.1 g of the resin was mixed with 200 mL of the buffer solution at different pH values. After saturation, filtered and weighed, the hydrogel characteristics were determined, and the absorbency was calculated.

2.5. Determination of biodegradability

Resin sheets measuring 1 cm × 2 cm were weighed and labeled separately. The sheets were then placed in 18 PDA plates containing mycete (six plates each of *Penicillium*, *A. niger*, and *L. edodes*), sealed with tape, and incubated at 30 °C. Afterwards, the resin products were filtered, dried, weighed, and the biodegradation was observed every 3 days.

3. Results and discussion

3.1. Effects of synthesis conditions on the water absorption properties of the resin

Fig. 1(a) shows that the increase in the mass ratio of AA:AM caused an increase in the swelling capacity of the resin. When the mass ratio of AA:AM was 7:1, the swelling capacity was relatively high and the gel strength was good. The increase in the concentration of acrylic acid favors the movement of ion groups into the resin. The osmotic pressure inside the resin increases accordingly and facilitates the penetration of water molecules into the interior of the resin upon contact with water. Moreover, the repulsion of the ion groups that were relocated inside the resin toward one another promotes swelling. Further increase of the AA content resulted in the increase in ionic group content inside the resin. However, the water absorbance was less because the absorption properties of the resin did not solely rely on osmotic pressure as a consequence of the ionic groups, but also due to the synergistic interaction between the various groups in the resin.

Fig. 1(b) shows that the reaction time greatly influences the water absorbency of the resin, which increases with time. When the reaction time was 4 h, the resin water absorbency in distilled water was 1083.9 g/g, and 95.62 g/g in 0.9 wt.% NaCl. At a reaction time of 5 h, the resin water absorbency decreased. These observations are in line with the free radical reaction rule, which states that if the reaction time is too short, polymerization does not proceed to completion and results in low relative molecular mass and small network size after swelling with low resin water absorbency. Therefore, the prolonged reaction time can increase the degree of polymerization at the beginning of the reaction. Steady-state polymerization was reached after 4 h of reaction. In this stage, the generation rate of the free radical is equal to its consumption rate, which establishes a dynamic equilibrium wherein the reaction time has no influence on water absorbency. On the other hand, a very long reaction time causes the degradation of resin and results in a low molecular weight (Xu, Li, & Sun, 2010). In addition, stirring causes shear stress in the reaction system for a long time, thereby decreasing its viscosity. The decrease in viscosity is not conducive to polymerization, therefore, decreases the water absorbency.

Fig. 1(c) shows that the increase in the concentration of the cross-linking agent NMBA resulted in the initial increase, and then

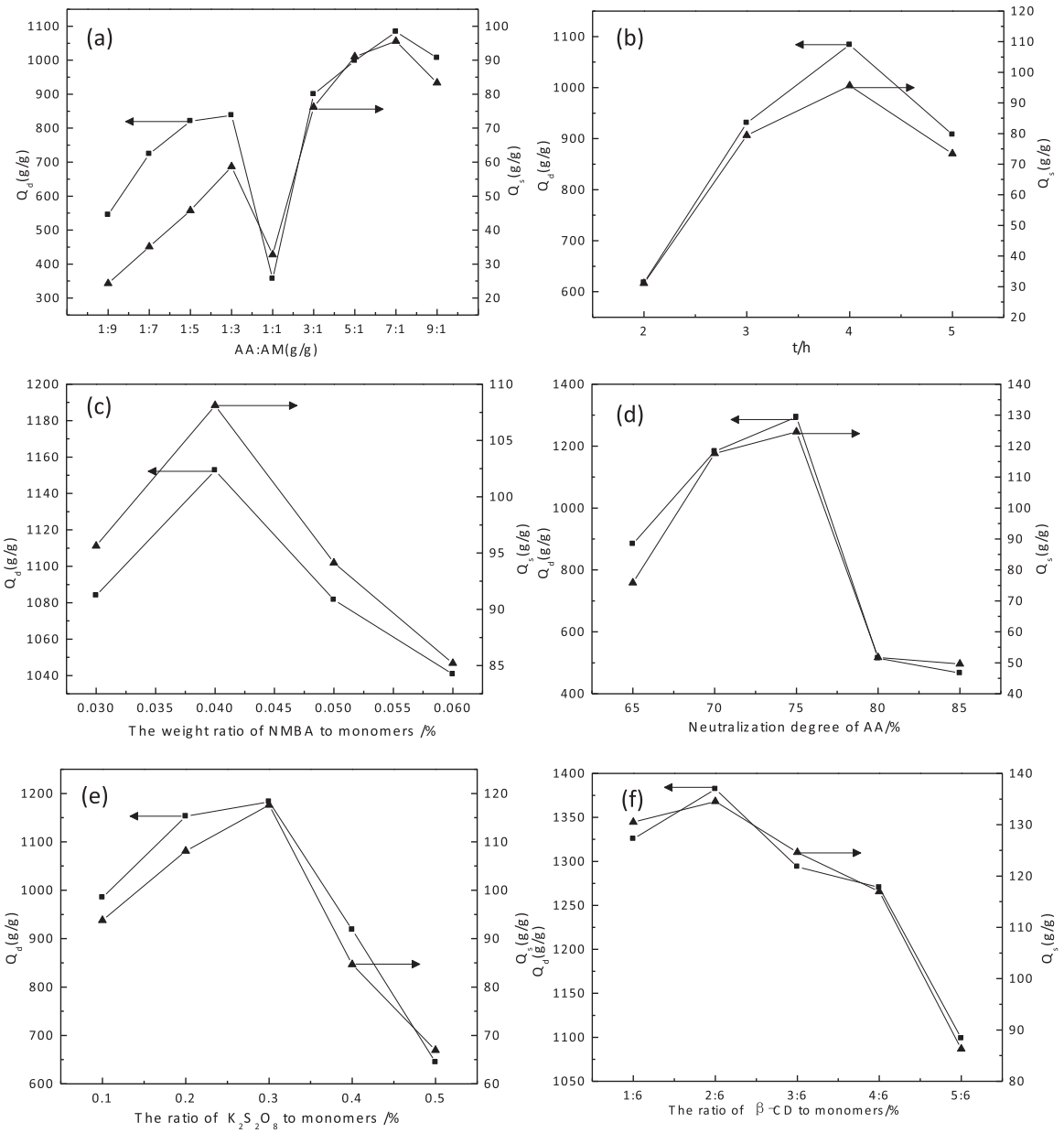

Fig. 1. Effects of the experimental conditions on water absorption capacities.

decrease of the swelling capacity of the resin. This result was observed because when the cross-linker concentration is too low, the cross-linking density of the resin would also be low, which causes the formation of a sparse three-dimensional network that facilitates water entry. Moreover, the adsorption ability decreased, and the solubility of the material increased on a macroscopic perspective, which led to a decrease in water absorbency. This decrease has direct effects on the hydrogel strength after swelling. The resin did not become an elastic gel but a colloid with low strength. The swelling ability of the resin was reduced. However, when the cross-linker concentrations are too high, the reaction activity of the cross-linker NMBA would also be high, with enough trace amounts of NMBA to facilitate cross-linking reactions and form a mesh structure (Peng, Xu, Peng, Wang, & Zheng, 2008; Pourjava, Barzegar, & Mahdavinia, 2006). The increase in cross-linking sites and cross-linking density makes the resin network distances closer and the resin hard to stretch, which result in the reduction of the volume of liquid it can hold and the reduction of swelling capacity. Considering the resin water absorbency and hydrogel state results, the cross-linker concentration was found to account for 0.04% of the total monomer mass at optimal experimental conditions.

As the neutralization degree of AA increased (Fig. 1(d)), the swelling capacity of the resin increased, and then decreased thereafter. This result was observed because the increase in neutralization degree led to an increase in the concentration of —COO^- on the resin surface. The atomic oxygen of —COO^- has coordination effects on heavy metal ions and is capable of chelation, which improve the adsorption capacity of the resin. The increase in neutralization leads to an increase in —COONa ion concentration in the reaction system. The dissociation of COONa into —COO^- in water is much more favored. The dissociation of —COOH increases in —COONa and leads to more —COO^-. More carboxylic acid anions on the network chain made the chain more stretchable. In addition, the repulsion between and among different chains is enhanced. The water absorbency increases as the force caused by chain expansion in the network increases (Pourjava & Amini-Fazl, 2007). However,

when the neutralization degree is too high, the Na^+ concentration on the network of graft copolymers being formed increases, and the electrostatic repulsion between charges causes the contact of the heavy metal and coordination groups on the surface of the resin and chelate formation difficult. The excess in the degree of neutralization is not conducive to resin adsorption. However, with the increase in the neutralization degree, the shielding effect of Na^+ on the carboxylic acid anion in the system gradually appears, which weakens the repulsion among the chains or adjacent carboxylic acid anions on the same chain and reduces the extension driving force of the network. Therefore, when the neutralization degree is too high, the swelling capacity is reduced.

The selection of the initiator and the dosage directly affects the reaction process and its results. Dosage determines the number of active sites in a system, which affects the reaction rate. The reaction rate is a very important factor for controlling experiments (Ma et al., 2011). Fig. 1(e) shows the effect of the initiator dosage on the resin absorption rate in distilled water and salt solutions. Furthermore, as the initiator concentration was increased, the absorbency of the resin, both in distilled water and salt solutions, initially increased, and decreased thereafter. When the initiator dosage accounted for 0.3% of the total monomer, the water absorbency of the resin for both distilled water and 0.9 wt.% NaCl was the highest at 1183 g/g and 117.6 g/g, respectively. Lower dosages result in a very few active sites in the reaction system, which do not allow the resin to form an effective three-dimensional cross-linked structure. On the other hand, when the initiator dosage is very high, the polymerization reaction becomes too fast and the resin forms a three-dimensional space structure with many branched chains. This resin has a poor water absorbency. Therefore, choosing the right initiator dosage is important. In the current experiment, the optimal initiator dosage for resin formation accounts for 0.3% of the total weight of the monomer.

Fig. 1(f) shows the effect of β-CD use on resin absorbency. The primary role of β-CD is to provide a skeleton of cross-linked network. In addition, β-CD also contributes to the promotion of polymerization (Peng et al., 2008). β-CD dosage is 10–30% of the monomer weight. Fig. 1(f) further reveals that water absorbency initially increased and then decreased with increasing β-CD dosages. When the mass ratio of β-CD to the monomers was 2:6, the best swelling performance of the resin was observed. The water absorbency in distilled water was 1382.11 g/g and that in 0.9 wt.% NaCl was 129.54 g/g. If the dosage of β-CD was too low, the AA and AM concentrations would have been relatively too much and the cross-linking degree would have been too high, which result in a low water absorbency of resin. When the β-CD dosage is too high, the resin water absorbency decreases with increasing β-CD dosage because the dosage of AA and AM, as well as the cross-linking, is relatively too low, which results in a decline in water absorbency. In addition, graft polymerization could not completely occur at very high dosages, and the products are soluble in water, which result in a low-strength hydrogel.

3.2. FTIR spectra analysis

The FTIR spectra of β-CD and the resin are shown in Fig. 2. The strong and wide —OH peak for β-CD at 3404 cm^{-1} moved toward a lower wave number, and the resin had a strong and broad absorption peak at 3363 cm^{-1} (Ficarra et al., 2002). The introduction of acrylic acid increased —OH, which led to the shift of the —OH peak toward a lower wave number. Furthermore, the —OH group absorption peak became broader because of the increasing hydrogen bonding between molecules. The $—CH_2$ stretching vibrations at 2925 cm^{-1} and 2846 cm^{-1} were significantly increase for the resin, which is mainly due to the formation of $—CH_2$ in the polymerization process during the introduction of acrylic acid and

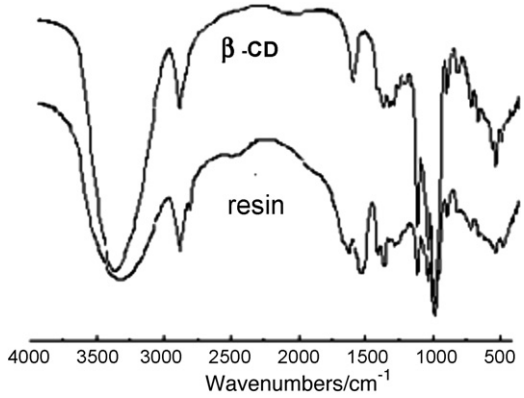

Fig. 2. FTIR spectra of β-CD and resin.

acrylamide monomer. Strong overlapping peaks at 1671 cm^{-1} can be attributed to —C=O stretching vibration peaks in acrylamide and carboxylic acids (Kuang, YuK, & Huh, 2011). The strong stretching vibration peak at 1570 cm^{-1} was the N–H absorption peak in the acylamino group. The asymmetric stretching vibration peak of the carbonyl group of —COONa in sodium polyacrylate was observed at 1451 cm^{-1}, whereas the strong bands at 1410 cm^{-1} were either a stretching vibration peak for C–N or a bending vibration peak for $—CH_2—$, which indicates the presence of acylamino groups in the resin (Huang, Liu, Zhang, Xu, & Hu, 2012). Based on these results, we can conclude that carboxyl and amide groups were introduced to the resin products, and the lack of a characteristic —C=C absorption peak indicates that a polymerization reaction occurred between β-CD, AA, and AM.

3.3. Morphological analyses

Fig. 3 shows the SEM images of the resin incubated in different liquid media. The SEM images of the dry resin surface and the cross section are shown in Fig. 3(a) and (b). From Fig. 3(b), the resin produced through graft copolymerization of β-CD with AA and AM had a clear, stratified rock structure with a large number of pores (Fig. 3(b)), which increased the adsorption surface area and improved the exchange and adsorption processes. The SEM images of the resin in distilled water and in NaCl, $CaCl_2$, and $AlCl_3$ solutions are shown in Fig. 3(c)–(f), respectively. After absorption, the internal structure of the resin assumes an obvious three-dimensional polygon network on the inside, while the network size decreased with increasing valence state of the metal ions. The three-dimensional network structure of the resin in Ca^{2+} and Al^{3+} solutions was damaged to a particular degree. This observation is related with the swelling behavior of resin in high-state positive ion solutions. The swelling capacity also decreased with increasing valency of the metal ions.

3.4. Time-dependent swelling behaviors in chlorine saline solution

Fig. 4 shows the swelling curves of resin in NaCl, $CaCl_2$, and $AlCl_3$ solutions at different concentrations. In all these solutions at different concentrations, the resin swelling curve revealed that as the absorption time increased, the swelling capacity decreased with increasing valency of the metal ion and concentration of chloride in the solution. However, with the absorption time increased, the curves for $CaCl_2$ and $AlCl_3$ initially rapidly increased, then decreased, and finally leveled compared with the curve of the resin in NaCl. This trend reflects the swelling behavior, and no swelling observed in the NaCl solution. A large number of interconnected

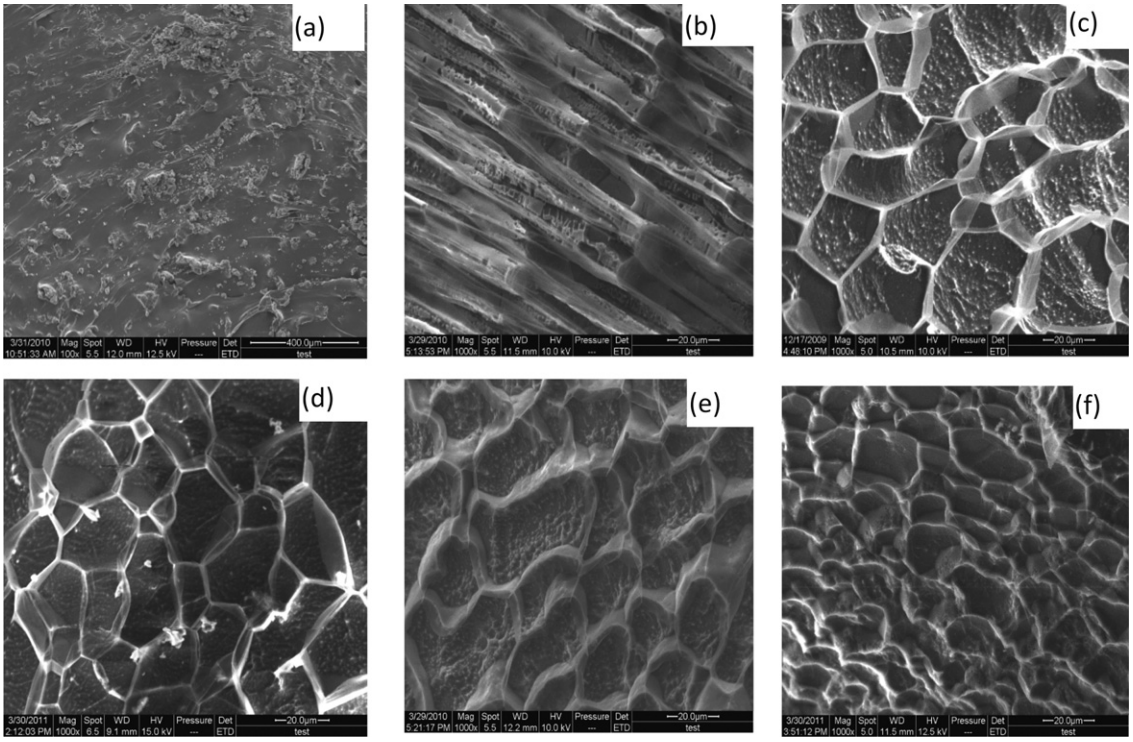

Fig. 3. SEM micrographs of (a, b) resin, (c) in distilled water, (d–f) in 0.01 mol/L NaCl, $CaCl_2$, and $AlCl_3$ solution, respectively.

openings in the resin enable the entry of an external solution to become easier. In the early phase of liquid absorption, the resin network expanded more. When the swelling reaches a particular extent, the network expansion power became much smaller, and the complexing action of —COO^- on the resin graft chains with bivalent and trivalent metal cation causes the graft chains that cross-link the resin network structure to shrink (Pourjavadi, Amini-Fazl, & Hosseinzadeh, 2005; Hua & Wang, 2009). This result leads to the leakage of absorbed water; thus, a maximum in swelling with time was observed (Wang & Wang, 2010). The stability constant order of the complexes produced by bivalent and trivalent metal ions with —COO^- is greater for Ca^{2+} than in Al^{3+} because the stability of the complexes formed by bivalent and trivalent metal cations with the resin is much higher than that by monovalent cations (Zhao, Su, Fang, & Tan, 2005). The resin in bivalent and trivalent metal cation solutions exhibits overswelling. The ionic radius of Na^+ is smaller than that of Ca^{2+} and Al^{3+} at the same plasma strength conditions, and the swelling capacity of the resin in Na^+ is higher than in Ca^{2+} and Al^{3+}. At concentrations from 0.01 mol/L to 0.1 mol/L, the swelling capacity of the resin was highest in NaCl ($NaCl > CaCl_2 > AlCl_3$).

3.5. Effects of pH

Fig. 5 shows the moisture absorption of the resin in buffer solutions with different pH values. The pH significantly affects the swelling capacity of the resin. When the pH was less than 2, the resin almost did not swell. From pH 2 to 6, water absorbency rapidly increased with increasing pH. At pH 6–12, the swelling capacity was almost constant. In strong acidic conditions, most —COO^- in the three-dimensional network chain of resin exists as —COOH (Wang & Wang, 2010). This result lowers the repulsion power of the three-dimensional network chains; therefore, the swelling capacity is very low at low pH conditions. The —COO(H) in resin chains mainly exists as —COO^- in high pH conditions, and the hydrogel network chains are mutually exclusive. The swelling capacity greatly

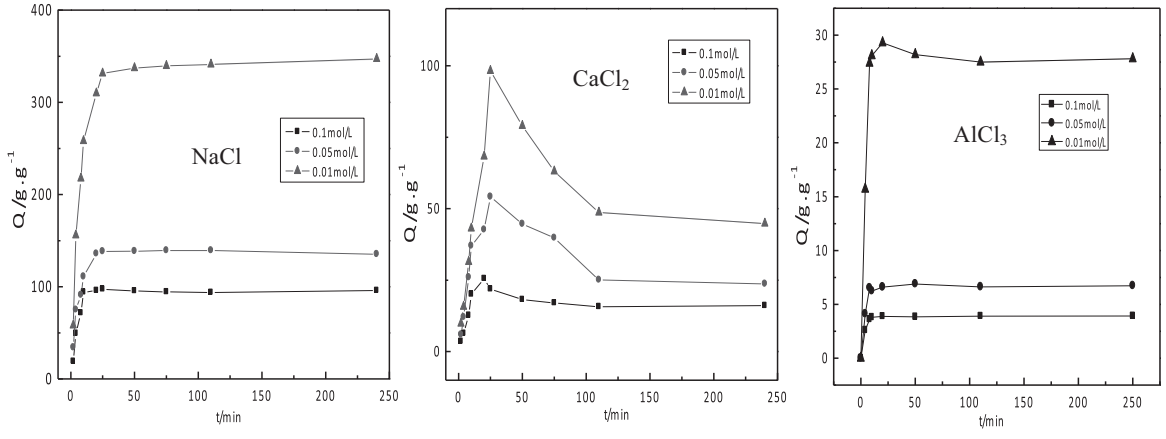

Fig. 4. Kinetic swelling curves of the polymer in different chlorine saline solutions.

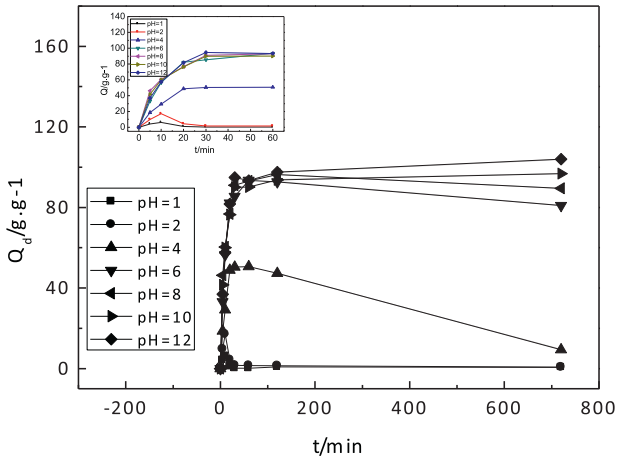

Fig. 5. Effects of pH on water absorption capacity.

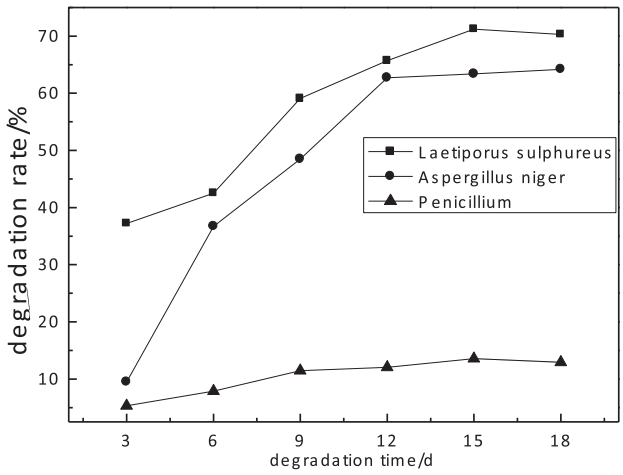

Fig. 7. Mycete degradation of resin.

increases because of the osmotic difference and hydrogen bonding between ions and the expansion of mesh space after the formation of a large envelope of water (Zhao et al., 2005). The osmotic difference decreases and retraction forces increase with increasing swelling capacity, which then limits the amount of water that can enter the network. When equilibrium is reached, the swelling capacity becomes constant.

3.6. Analysis of differential scanning calorimetry

The DSC curve for resin in a temperature-dependent heat flow is shown in Fig. 6. Two broad and weak exothermic peaks can be observed at 320 °C and 373 °C. The graft polymerization and molecular weight of the resin were high, which imply that a high temperature is required to change the resin morphology. The exothermic peaks observed were caused by the heat produced during the transformation of resin from solid to a highly elastic state (Giammona, Gavallaro, Maniscalco, Craparo, & Pitarresi, 2006). The exothermic peak of the resin had a wide peak shape and revealed a wide range of molecular weights, which indicate that the resin is made up of different polymers of various molecular weights (Stark & Jaunich, 2011). Two strong and sharp exothermic peaks at 427 °C and 464 °C disappeared above 400 °C, which indicates that the resin transformed from being highly elastic into either a viscous phase or a more rigid phase. The resin is thermoplastic because it can transform from highly elastic to a more viscous state at high temperatures (Ficarra et al., 2000). As shown in Fig. 4, the resin is stable

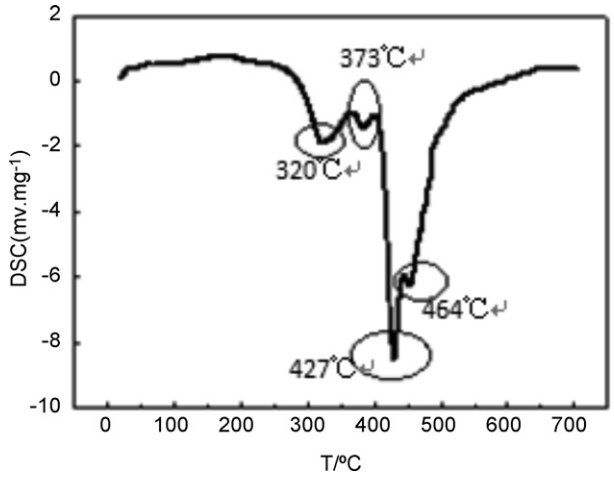

Fig. 6. The DSC of the resin.

below 300 °C where it does not undergo decomposition or state changes (Voncina, Majcen, & Marechal, 2005).

3.7. Biodegradation of resin

The degradation efficiencies of the resin gel in *Penicillium*, *A. niger*, and *L. edodes* are shown in Fig. 7. The degradation was observed to be very slow with *Penicillium* with only 5.4% of the resin gel was degraded after 3 days and 8.9% after 10 days. The degradation efficiency reached a maximum at 13.5% after 20 days. *Penicillium* almost did not grow in the resin. After 20 days, the resin samples were able to keep their original shape. In *A. niger*, the resin gel degradation efficiency rapidly increased with time. After 3 days, the degradation efficiency was just 9.6%, but in day 12, it was 62.7% and reached 64.2% after 18 days. *A. niger* grew abundantly in the resin, and the shape of the samples changed (no longer a rectangle). With *L. edodes*, the degradation efficiency reached 37.2% after 3 days, and 71.2% after 18 days. And, in day 3, the block samples turned into fluid. These results demonstrate that *L. edodes* degrades better than the other mycetes, and that the resin gel is biodegradable. The ranking of the mycete based on the influence on resin degradation efficiency is as follows: *L. edodes* > *A. niger* > *Penicillium*. The results also indicate that microorganisms degrade some of the resin components. The observations that the mycete attach to the resin surface and produce various enzymes imply that the organisms could enter the active sites of resin macromolecules and penetrate into the functional points of the polymer. The resin gel that was contaminated by microorganisms such as fungi and bacteria gradually disappeared. The pores that were formed in the polymer during contamination mechanically weakened the structure of the material. The skeletal macromolecules may incur fractures in some chain segments, which may eventually lead to its degradation to smaller and more stable molecular products; therefore, facilitating further natural decomposition (Kuang et al., 2011). This result further shows that the polymer is an eco-friendly material.

4. Conclusions

This study used the polyhydroxy structure of β-CD for the synthesis of β-cyclodextrin-based resin with super water absorbency. In this optimized condition, the water absorbency of the resin was 1544.76 g/g in distilled water and 144.52 g/g in 0.9 wt.% NaCl. Significant overswelling of the resin occurred in $CaCl_2$ and $AlCl_3$ solutions. The synthesized resin (dry) exhibited a clear stratified rock structure and had a large number of pores. The interior of the resin

hydrogel showed a polygon structure with a three-dimensional network structure. The resin was thermoplastic, pH-sensitive, and biodegradable. This paper is merely a preliminary work. Further research on the role of resin in metal ion elimination will be conducted to explore other possible application of this material.

Acknowledgments

This research was supported by the National Natural Science Foundation of China (Grant No. 31000277) and the Central University Basic Scientific Research Project of China (Grant No. DL11EB01). The authors are grateful for the financial support of the National Department Public Benefit Research Foundation (Grant No. 200904072) and the Ph.D. Programs of Foundation of the Ministry of Education of China (Grant No. 20100062120005).

References

Abedi-Koupai, J., Eslamian, S. S., & Asadkazemi, J. (2008). Enhancing the available water content in unsaturated soil zone using hydrogel to improve plant growth indices. *Ecohydrology & Hydrobiology*, *8*, 67–75.

Banerjee, S. S., & Chen, D. H. (2010). Grafting of 2-hydroxypropyl-β-cyclodextrin on gum arabic-modified iron oxide nanoparticles as a magnetic carrier for targeted delivery of hydrophobic anticancer drug. *International Journal of Applied Ceramic Technology*, *7*, 111–118.

Bhardwaj, A. K., Shainberg, I., Goldstein, D., Warrington, D. N., & Levy, G. J. (2007). Water retention and hydraulic conductivity of cross-linked polyacrylamides in sandy soils. *Soil Science Society of America Journal*, *71*, 406–412.

Buchholz, F. L. (1996). Superabsorbent polymer: an idea whose time has come. *Journal of Chemical Education*, *73*, 512–515.

Chang, C. Y., Duan, B., Cai, J., & Zhang, L. (2010). Superabsorbent hydrogels based on cellulose for smart swelling and controllable delivery. *European Polymer Journal*, *46*, 92–100.

Cobos Cruz, L. A., Martinez Perez, C. A., Monreal Romero, H. A., & Garcia Casillas, P. E. (2007). Synthesis of magnetite nanoparticles–β-cyclodextrin complex. *Journal of Alloys and Compounds*, *466*, 330–334.

Dell Valle, E. M. M. (2004). Cyclodextrins and their uses: a review. *Process Biochemistry*, *39*, 1033–1046.

Ficarra, R., Ficarra, P., Di Bella, M. R., Raneri, D., Tommasini, S., Calabrò, M. L., et al. (2000). Study of β-blockers/β-cyclodextrins inclusion complex by NMR, DSC, X-ray and SEM investigation. *Journal of Pharmaceutical and Biomedical Analysis*, *23*, 33–40.

Ficarra, R., Tommasini, S., Raneri, D., Calabrò, M. L., Di Bella, M. R., Rustichelli, C., et al. (2002). Study of flavonoids/β-cyclodextrin inclusion complexes by NMR, FTIR, DSC, X-ray investigation. *Journal of Pharmaceutical and Biomedical Analysis*, *29*, 1005–1014.

Giammona, G., Cavallaro, G., Maniscalco, L., Craparo, F. E., & Pitarresi, G. (2006). Synthesis and characterization of novel chemical conjugates based on α,β-polyaspartylhydrazide and β-cyclodextrins. *European Polymer Journal*, *42*, 2715–2729.

Guo, M. Y., & Jiang, M. (2007). Macromolecular self-assembly based on inclusion complexation of cyclodextrins. *Progress in Chemistry*, *19*, 557–566.

Han, Y. G., Yang, P. L., & Luo, Y. P. (2010). Porosity change model for watered super absorbent polymer-treated soil. *Environmental Earth Sciences*, *61*, 1197–1205.

Hua, S. B., & Wang, A. Q. (2009). Synthesis, characterization and swelling behaviors of sodium alginate-g-poly(acrylic acid)/sodium humate superabsorbent. *Carbohydrate Polymers*, *75*, 79–84.

Huang, Z. H., Liu, S. X., Zhang, B., Xu, L. L., & Hu, X. F. (2012). Equilibrium and kineti-cs studies on the absorption of Cu(II) from the aqueous phase using a <beta>-cyclodextrin-based adsorbent. *Carbohydrate Polymers*, *88*, 609–617.

Kabiri, K., Omidian, H., Hashemi, S. A., & Zohuriaan-Mehr, M. J. (2003). Synthesis of fast-swelling superabsorbent hydrogels: effect of crosslinker type and concentration on porosity and absorption rate. *European Polymer Journal*, *39*, 1341–1348.

Kuang, J., YuK, K. Y., & Huh, K. M. (2011). Polysaccharide-based superporous hydrogels with fast swelling and superabsorbent properties. *Carbohydrate Polymers*, *83*, 284–290.

Liu, C. Y., Zhang, M. J., & Zhu, J. (2008). Synthesis and characterization of a saltresisting superabsorbent based on poly(acrylic acid) with sodium tungstate as a crosslinker. *Journal of Applied Polymer Science*, *110*, 2440–2445.

Ma, Z. H., Li, Q., Yue, Q. Y., Gao, B. Y., Xu, X., & Zhong, Q. Q. (2011). Synthesis and characterization of a novel super-absorbent based on wheat straw. *Bioresource Technology*, *102*, 2853–2858.

Peng, G., Xu, S. M., Peng, Y., Wang, J. D., & Zheng, L. C. (2008). A new amphoteric superabsorbent hydrogel based on sodium starch sulfate. *Bioresource Technology*, *99*, 444–447.

Pourjava, A., & Amini-Fazl, M. S. (2007). Optimized synthesis of carrageenan graft-poly(sodium acrylate) super-absorbent hydroxyl using the Taguchi method and investigation of its metal ion absorption. *Polymer International*, *56*, 283–289.

Pourjava, A., Barzegar, S., & Mahdavinia, G. R. (2006). MBA-cross-linked Na-Al_g/CMC as a smart full-polysaccharide super-absorbent hydrogels. *Carbohydrate Polymers*, *66*, 386–395.

Pourjavadi, A., Amini-Fazl, M. S., & Hosseinzadeh, H. (2005). Partially hydrolyzed crosslinked alginate-graft-polymethacrylamide as a novel biopolymer-based superabsorbent hydrogel having pH-responsive properties. *Macromolecular Research*, *13*, 45–53.

Silberbush, M., Adar, E., & De, M. Y. (1993). Use of all hydropholie polymer to improve water storage and availability to crops grown in sand dunes. *Agricultural Water Management*, *23*, 303–313.

Stark, W., & Jaunich, M. (2011). Investigation of ethylene/vinyl acetate copolymer (EVA) by thermal analysis DSC and DMA. *Polymer Testing*, *30*, 236–242.

Sun, L. P., Du, Y. M., Shi, X. W., Chen, X., Yang, J. H., & Xu, Y. M. (2006). A new approach to chemically modified carboxymethyl chitosan and study of its moisture-absorption and moisture-retention abilities. *Journal of Applied Polymer Science*, *102*, 1303–1309.

Szejtli, J. (1998). Introduction and general overview of cyclodextrin chemistry. *Chemical Reviews*, *98*, 1743–1754.

Voncina, B., Majcen, A., & Marechal, L. (2005). Grafting of cotton with β-cyclodextrin via poly(carboxylic acid). *Journal of Applied Polymer Science*, *96*, 1323–1328.

Wang, L., Zhang, J., & Wang, A. (2008). Removal of methylene blue from aqueous solution using chitosan-g-poly (acrylic acid)/montmorillonite superadsorbent nanocomposite. *Colloids and Surfaces A: Physicochemical and Engineering Aspects*, *322*, 47–53.

Wang, W. B., & Wang, A. Q. (2010). Synthesis and swelling properties of pH-sensitive semi-IPN superabsorbent hydrogels based on sodium alginate-g-poly(sodium acrylate) and polyvinylpyrrolidone. *Carbohydrate Polymers*, *80*, 1028–1036.

Xu, J., Li, X., & Sun, F. (2010). Cyclodextrin-containing hydrogels for contact lenses as a platform for drug incorporation and release. *Acta Biomaterialia*, *6*, 486–493.

Yao, K. J., & Zhou, W. J. (2003). Synthesis and water absorbency of the copolymer of acrylamide with anionic monomers. *Journal of Applied Polymer Science*, *53*, 1533–1538.

Zhang, J. P., & Li, A. (2005). Study on superabsorbent composite: synthesis, swelling behaviors and application of poly (acrylic acid-co-acrylamide)/sodium humate/attapulgitesuperabsorbent composite. *Polymers for Advanced Technologies*, *16*, 813–820.

Zhao, Y., Su, H. J., Fang, L., & Tan, T. W. (2005). Superabsorbent hydrogels from poly(aspartic acid) with salt-,temperature- and pH-responsiveness properties. *Polymer*, *46*, 5368–5376.